

PURDUE UNIVERSITY
GRADUATE SCHOOL
Thesis/Dissertation Acceptance

This is to certify that the thesis/dissertation prepared

By Eunhye Cho

Entitled

EFFECTS OF INTERSTITIAL FLUID FLOW AND CELL COMPRESSION IN FAK AND SRC
ACTIVITIES IN CHONDROCYTES

For the degree of Master of Science in Biomedical Engineering

Is approved by the final examining committee:

Sungsoo Na

Chair

Hiroki Yokota

Jiliang Li

To the best of my knowledge and as understood by the student in the *Research Integrity and Copyright Disclaimer (Graduate School Form 20)*, this thesis/dissertation adheres to the provisions of Purdue University's "Policy on Integrity in Research" and the use of copyrighted material.

Approved by Major Professor(s): Sungsoo Na

Approved by: Edward J. Berbari

Head of the Graduate Program

04/08/2013

Date

EFFECTS OF INTERSTITIAL FLUID FLOW AND CELL COMPRESSION
IN FAK AND SRC ACTIVITIES IN CHONDROCYTES

A Thesis

Submitted to the Faculty

of

Purdue University

by

Eunhye Cho

In Partial Fulfillment of the

Requirements for the Degree

of

Master of Science in Biomedical Engineering

May 2013

Purdue University

Indianapolis, Indiana

ACKNOWLEDGMENTS

I would like to gratefully acknowledge my thesis advisor, Dr. Na, for his assistance, guidance, and supervision during the entire course of this research and thesis work. His research experience and pursuit of perfection even in details aided me in more ways than one. I would like to also thank my advisory committee members, Dr. Hiroki Yokota and Dr. Jiliang Li for their time and feedback during the completion of my thesis.

I am thankful to my co-worker, Qiaoqiao Wan, for her support in the laboratory. I extend my thanks to the assistance from Ms. Valerie Lim Diemer in formatting this thesis.

Lastly, I express my profound gratitude to my parents for their great support and encouragement during all my life, especially during this master degree course, and my sincere friends.

TABLE OF CONTENTS

	Page
LIST OF FIGURES	v
ABSTRACT	vii
1. INTRODUCTION	1
1.1 Osteoarthritis.....	1
1.2 Mechanical Loading and Chondrocyte Behavior	1
1.3 The Involvement of FAK and Src in Chondrocyte Behavior	3
1.4 Thesis Objectives	4
2. METHODS	6
2.1 DNA Plasmids.....	6
2.2 Fabrication of Type II Collagen-Conjugated Agarose Gel	7
2.3 Cell Maintenance and Transfection	8
2.4 Immunostaining and Microscopy	9
2.5 Preparation of Chondrocyte/Gel Constructs	10
2.6 Shear Flow Application and Microscopy.....	11
2.7 Data Analysis and Image Processing	13
2.8 Measurement of Cell Deformation under Flow	13
2.9 Statistical Analysis.....	14
3. RESULTS	15
3.1 $\beta 1$ Integrin Activation is Significantly Enhanced in Chondrocytes in AG-Col Gel.....	15
3.2 Cell Deforms Substantially in Simultaneous Cell Deformation/Interstitial Fluid Flow Region	17
3.3 FAK Activity in Response to Interstitial Fluid Flow	19
3.4 FAK Activity in Response to Simultaneous Cell Deformation/Interstitial Fluid Flow	21
3.5 Src Activity in Response to Interstitial Fluid Flow.....	23
3.6 Src Activity in Response to Simultaneous Cell Deformation/Interstitial Fluid Flow	25
3.7 Different Loading Type Does Not Affect the Loading Magnitude-Dependent FAK Activity	27

	Page
3.8 Different Loading Type Significantly Affects the Loading Magnitude-Dependent Src Activity	29
3.9 FAK and Src Behave Similarly under Interstitial Fluid Flow Only.....	31
3.10 Simultaneous Application of Cell Deformation and Interstitial Fluid Flow Leads to Differential FAK and Src Activities	33
4. DISCUSSION.....	35
LIST OF REFERENCES.....	39

LIST OF FIGURES

Figure	Page
Figure 2.1	7
Figure 2.2	11
Figure 2.3	12
Figure 3.1	16
Figure 3.2	18
Figure 3.3	20

Figure	Page
Figure 3.4 FAK activity is mechanical loading-magnitude dependent under simultaneous cell deformation and interstitial fluid flow. (A) 2 $\mu\text{l}/\text{min}$ ($n = 10$ cells), (B) 5 $\mu\text{l}/\text{min}$ ($n = 9$ cells), (C) 10 $\mu\text{l}/\text{min}$ ($n = 10$ cells), (D) 20 $\mu\text{l}/\text{min}$ ($n = 10$ cells). Scale bars: 10 μm	22
Figure 3.5 Src activity is mechanical loading-magnitude dependent under interstitial fluid flow only. (A) 2 $\mu\text{l}/\text{min}$ ($n = 4$ cells), (B) 5 $\mu\text{l}/\text{min}$ ($n = 10$ cells), (C) 10 $\mu\text{l}/\text{min}$ ($n = 7$ cells), (D) 20 $\mu\text{l}/\text{min}$ ($n = 10$ cells). Scale bars: 10 μm	24
Figure 3.6 Src activity is mechanical loading-magnitude dependent under simultaneous cell deformation and interstitial fluid flow region. (A) 2 $\mu\text{l}/\text{min}$ ($n = 10$ cells), (B) 5 $\mu\text{l}/\text{min}$ ($n = 8$ cells), (C) 10 $\mu\text{l}/\text{min}$ ($n = 8$ cells), (D) 20 $\mu\text{l}/\text{min}$ ($n = 10$ cells). Scale bars: 10 μm	26
Figure 3.7 Different loading type does not affect the loading magnitude-dependent FAK activity. Bar graphs represent maximal changes in FAK activity of the cells under interstitial fluid flow only (IFF; <i>white</i>) and simultaneous cell deformation and interstitial fluid flow (Cell deformation/IFF; <i>black</i>). The numbers under black bars represent cell deformation under the given flow rate. * $P < 0.05$. $n < 6$ cells.	28
Figure 3.8 Different loading type significantly affects the loading magnitude-dependent Src activity. Bar graphs represent maximal changes in Src activity of the cells under interstitial fluid flow only (IFF; <i>white</i>) and simultaneous cell deformation and interstitial fluid flow region (Cell deformation/IFF; <i>black</i>). * $P < 0.05$, **** $P < 0.0001$. $n > 4$ cells.....	30
Figure 3.9 FAK and Src behave similarly under interstitial fluid flow only. Bar graphs represent maximal changes in FRET activities of FAK and Src in the cells in interstitial fluid flow only. *** $P < 0.001$. $n > 4$ cells	32
Figure 3.10 Simultaneous cell deformation and interstitial fluid flow cause differential FAK and Src activities. Bar graphs represent maximal changes in FRET activities of FAK and Src in the cells in simultaneous cell deformation/interstitial fluid flow. *** $P < 0.001$, **** $P < 0.0001$. $n > 9$ cells.	34

ABSTRACT

Cho, Eunhye. M.S.B.M.E., Purdue University, May 2013. Effects of Interstitial Fluid Flow and Cell Compression in FAK and Src Activities in Chondrocytes. Major Professor: Sungsoo Na.

Articular cartilage is subjected to dynamic mechanical loading during normal daily activities. This complex mechanical loading, including cell deformation and interstitial fluid flow, affects chondrocyte mechano-chemical signaling and subsequent cartilage homeostasis and remodeling. Focal adhesion kinase (FAK) and Src are known to be main mechanotransduction proteins, but little is known about the effect of mechanical loading on FAK and Src under its varying magnitudes and types. In this study, we addressed two questions using C28/I2 chondrocytes subjected to the different types and magnitudes of mechanical loading: Does a magnitude of the mechanical loading affect activities of FAK and Src? Does a type of the mechanical loading also affect their activities? Using fluorescence resonance energy transfer (FRET)-based FAK and Src biosensor in live C28/I2 chondrocytes, we monitored the effects of interstitial fluid flow and combined effects of cell deformation/interstitial fluid flow on FAK and Src activities. The results revealed that both FAK and Src activities in C28/I2 chondrocytes were dependent on the different magnitudes of the applied fluid flow. On the other hand, the type of mechanical loading differently affected FAK and Src activities.

Although FAK and Src displayed similar activities in response to interstitial fluid flow only, simultaneous application of cell deformation and interstitial fluid flow induced differential FAK and Src activities possibly due to the additive effects of cell deformation and interstitial fluid flow on Src, but not on FAK. Collectively, the data suggest that the intensities and types of mechanical loading are critical in regulating FAK and Src activities in chondrocytes.

1. INTRODUCTION

1.1 Osteoarthritis

Osteoarthritis (OA) is the most common joint disorder that degrades articular cartilage. It has been known that the development of OA is induced by several factors such as age, sex, heredity, joint mechanics, and cartilage biology and biochemistry [1-3]. Pathologically, synovitis is considered to play a role in the progression of the cartilage degradation in OA, causing synovial hypertrophy and hyperplasia [4]. It leads to joint swelling, mononuclear cell infiltration, and synovial and subchondral angiogenesis. Cartilage degradation involves the destruction of collagen fibrils and proteoglycans induced by catabolic activity of various degradative enzymes such as the matrix metalloproteinase (MMP) and aggrecanase [5, 6].

1.2 Mechanical Loading and Chondrocyte Behavior

Chondrocytes are the only cell type present in the articular cartilage and their response to mechanical stimuli including cell/matrix deformation and interstitial fluid flow influences the maintenance and remodeling of the cartilage [7-11]. Within the cartilage tissue, common daily activities introduce complex mechanical stimuli to the chondrocytes such as compression, shear, and fluid flow as well as chemical or electrical

changes [12]. These factors are inherently coupled and their magnitudes are differently applied to the chondrocytes depending on the region of the tissue. Compression of cartilage tissue, for instance, simultaneously induces cell and matrix deformation and interstitial fluid flow in the surface region of the tissue [13]. Because these mechanical factors are closely linked to the cartilage homeostasis, identifying the role of the individual mechanical factors for regulating chondrocyte mechanotransduction will have important implications in cartilage health and disease. It has been shown that, compared to compression, direct shear application which induces chondrocyte deformation with negligible fluid flow results in different temporal activation levels of genes involved in matrix synthesis and degradation [8]. On the other hand, interstitial fluid flow also plays an important role in chondrocyte mechanotransduction. Interstitial fluid flow has been found to activate Ca^{2+} signaling of chondrocytes in three-dimensional (3D) alginate matrices [9, 14].

In addition to the effect of loading type, numerous studies have shown that the balance between anabolic and catabolic responses of the chondrocytes to mechanical loading is dependent on the loading intensities (reviewed in ref. [15]). Moderate, physiological loading, for instance, increases synthetic activity of the extracellular matrix (ECM) such as collagen type II, aggrecan, and proteoglycan [16-23], while decreasing the catabolic activity of degradative enzymes such as matrix metalloproteinases (MMPs) and ADAMTS (a disintegrin and metalloproteinase with thrombospondin motifs) [23-29]. In contrast to moderate loading, static or high-intensity loading has been shown to

degrade the cartilage resulting from inhibition of matrix synthesis and up-regulation of catabolic activities [27, 28, 30-32]. Therefore, the importance of these load-dependent signaling pathways involved in the maintenance and remodeling of the cartilage is widely accepted. However, the underlying mechanisms as to how varying magnitudes and types of mechanical stimuli trigger differential signaling activities that consequently lead to selective gene expression are not clear.

1.3 The Involvement of FAK and Src in Chondrocyte Behavior

Mechanical stimuli are believed to be sensed by the cell at the cell surface receptors such as integrins [33, 34]. When activated by mechanical loads, integrins undergo conformational changes [35, 36], and increase their affinity to extracellular matrix (ECM) proteins as well as various intracellular focal adhesion proteins [37]. This integrin activation by mechanical stimulation is known to be correlated with tyrosine phosphorylation of FAK and Src [38]. FAK and Src are considered to be the main mechanotransduction signaling proteins at the cell-ECM adhesion sites and their activities influence various structural and signaling changes within the cell, including cytoskeletal organization, migration, proliferation, differentiation, and survival [39]. Accumulating evidence has shown that integrin-mediated signaling activities through Src and FAK can regulate chondrocyte functions and pathology either cooperatively or independently. Src and FAK are known to form complexes, and lead to the activation of extracellular signal-regulated kinase (ERK) through mitogen-activated protein kinase (MAPK) signaling pathway [40]. ERK activation in chondrocytes by fluid flow [7] or

compression [9] has been reported to be associated with the regulation of both ECM gene expression and MMP activities. ERK activation by catabolic factor induces cartilage degradation and inhibition of ERK reduces MMP activities [41]. In addition to the linkage of Src and FAK to the regulation of ECM gene expression and MMP activities through MAPK signaling pathway, their activities are directly related to the cartilage pathology. It has been shown that FAK is up-regulated in both osteoarthritis and rheumatoid arthritis tissues [42]. FAK inhibition by siRNA transfection can decrease chondrocyte proliferation [43]. Src inhibition has also been reported to reduce chondrocyte proliferation and promote chondrogenic gene expression, thus maintaining chondrocyte phenotype [44]. Another study using rats with collagen-induced arthritis has shown that inhibiting Src can reduce cartilage degradation [45].

1.4 Thesis Objectives

The primary purpose of this study was to examine the activities of FAK and Src in chondrocytes in three-dimensional (3D) constructs while applying mechanical loading. In this study, we addressed two questions using chondrocytes subjected to the different types and magnitudes of mechanical loading: Does a magnitude of the mechanical loading affect activities of FAK and Src? Does a type of the mechanical loading also affect their activities? Using fluorescence resonance energy transfer (FRET)-based FAK and Src biosensor in live C28/I2 chondrocytes, we monitored the effects of interstitial fluid flow and combined effects of cell deformation/interstitial fluid flow on FAK and Src activities. During the imaging, four different magnitudes of fluid flow rates (2, 5, 10, and 20 $\mu\text{l}/\text{min}$)

were applied to visualize the activities of FAK and Src in the cells. We also monitored their activities in response to different loading types (i.e., interstitial fluid flow only, and simultaneous cell deformation/interstitial fluid flow). The role of collagen crosslinking on the activation of $\beta 1$ integrins was evaluated by comparing with two control matrices: agarose-only gels and agarose gels mixed with type II collagen without crosslinker.

2. METHODS

2.1 DNA Plasmids

Genetically encoded Src and FAK biosensors were used in this study to monitor the activities of Src or FAK in live C28/I2 cells. They were previously developed and their specificity has been well characterized as described [46-48]. FAK and Src biosensors consist of a Src SH2 domain, a specific tyrosine-containing substrate sequence, and a pair of cyan fluorescent protein (CFP) and yellow fluorescent protein (YFP) (Fig. 2.1). The substrates of the FAK and Src biosensors were derived from and the tyrosine 397 FAK auto-phosphorylation site [47], and p130Cas [46], respectively. The SH2 domain and the substrate are connected by a flexible linker. The SH2 domain is associated with CFP, and the substrate with YFP. CFP and YFP act as a donor and acceptor for FRET, respectively. When FAK or Src is not activated, CFP and YFP of the biosensor are in close proximity, and the excitation of CFP leads to a strong FRET from CFP to YFP. Upon activation of FAK or Src, the substrate of the specific biosensor is phosphorylated, and the subsequent intramolecular binding of the phosphorylated substrate to the Src SH2 domain leads to a conformational change of the biosensor, which results in a decrease of FRET. Thus, the activity of Src or FAK can be represented by the changes in FRET between CFP and YFP.

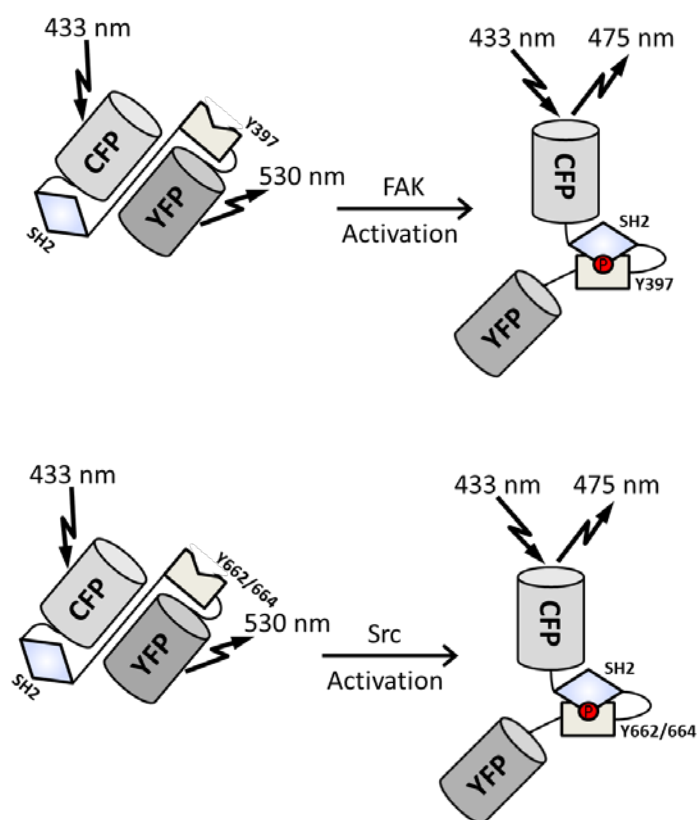


Figure 2.1 FAK and Src biosensors

2.2 Fabrication of Type II Collagen-Conjugated Agarose Gel

Collagen stock solution (1200 $\mu\text{g/ml}$) was prepared by dissolving type II collagen (Sigma, St.Louis, MO, USA) in 0.1 M acetic acid (Sigma), adjusting the pH to 7.4 with 1 M NaOH, and diluting in $\text{Ca}^{2+}/\text{Mg}^{2+}$ -free PBS. *N*-Sulfosuccinimidyl-6-(4'-azido-2'-nitrophenylamino) hexanoate (Sulfo-SANPAH) was used to conjugate type II collagen and agarose [49, 50]. Briefly, sulfo-SANPAH (Thermo Scientific, Waltham, MA,

USA) was added to the collagen solution and the collagen/crosslinker solution was incubated in the dark for 4 h at room temperature. Agarose solution was prepared by dissolving low melting temperature agarose (Sigma) in $\text{Ca}^{2+}/\text{Mg}^{2+}$ -free PBS, and sterilizing by autoclaving. Three parts 4 % agarose solution (w/v) was mixed with one part collagen/crosslinker solution. The mixture (3 % agarose and 300 $\mu\text{g}/\text{ml}$ collagen type II) was exposed to ultraviolet light (360 nm) for 15 min to activate the photoreactive groups of the sulfo-SANPAH and promote crosslinking reaction. The collagen-conjugated agarose (AG-Col) solution was then gelled at 4 °C at for 20 min and extensively washed in PBS for 3 days to remove the uncoupled proteins and crosslinker. The two control gels were prepared to examine the activation of $\beta 1$ integrins in chondrocytes: Agarose-only gels (AG) were prepared without the addition of collagen and crosslinker, and agarose gels mixed with collagen (AG+Col) were prepared without the addition of crosslinker.

2.3 Cell Maintenance and Transfection

C28/I2 human chondrocytes [51] were cultured in Dulbecco's Modified Eagle's Medium (DMEM; Lonza, Walkersville, MD, USA) containing 10% FBS (Hyclone, South Logan, UT, USA) and 1% antibiotics (50 units/ml penicillin and 50 $\mu\text{g}/\text{ml}$ streptomycin; Lonza, Basel, Switzerland). Prior to experiments, the cells were maintained at 37°C and 5% CO₂ in a humidified incubator. The DNA plasmids were transfected into the cells using a Neon transfection system (Invitrogen, Carlsbad, CA, USA), following the manufacturer's

protocol. A single, 1000 mV pulse with duration of 20 ms was found to be optimum for transfection. After transfection, the cells were transferred and mixed to liquefied type II collagen-conjugated agarose gel (AG-Col). The mixture was injected into a μ -slide cell culture chamber (Ibidi, Verona, WI, USA) and incubated in DMEM containing 0.5% FBS for 24-36 h before imaging experiments.

2.4 Immunostaining and Microscopy

C28/I2 cells were mixed with AG, AG+Col, and AG-Col gels, and 20 μ l of the mixture was transferred to a top-cut syringe. The gels were incubated for ~ 15min at room temperature to allow gelling. The cells seeded in gels samples were cultured in 48-well culture plates for 24-36 h. The cells were fixed with 4 % paraformaldehyde for 45 min at room temperature. After rinsing twice in PBS for 10 min on a platform shaker (Lonza), the cells were permeabilized with 0.5 % Triton X-100 (Sigma) in PBS for 45 min at room temperature. The samples were then incubated in blocking buffer (5% BSA, serum, 20 % Polyvinylpyrrolidone (Amresco, Solon, OH, USA) in PBS combined into 1:1:1 ratio) overnight at 4 °C on a rocking shaker. The samples were incubated with primary antibodies against activated β 1 integrin (1:500; Millipore, Billerica, MA, USA), or total β 1 integrin (1:100; Santa Cruz Biotechnology, Dallas, TX, USA) overnight at 4 °C, and washed overnight at 4 °C. The samples were then incubated with Alex Fluor 488 anti-mouse IgG (1:1000; Invitrogen) overnight at 4 °C. After washing, the samples were incubated in DAPI (Sigma) to visualize cell nuclei for 1 h and washed for 30 min three times at room temperature using a platform shaker.

An Olympus Fluoview FV1000 confocal microscope was used to visualize activated and total $\beta 1$ integrins and nuclei as well as actin cytoskeleton in cell/gel constructs. The fluorescence images were selected randomly, and then the fluorescence signal was quantified by measuring average intensity in individual cells using Fluoview Viewer software (Olympus). Images were acquired using a 60x objective lens (1.2 numerical aperture; Olympus).

2.5 Preparation of Chondrocyte/Gel Constructs

To make chondrocytes/gel constructs, two parts collagen-conjugated agarose gels (3 % agarose and 300 $\mu\text{g}/\text{ml}$ collagen type II) were melted at 50 °C for 30 min and mixed with one part 3x DMEM without FBS, resulting in 2 % agarose gels with 200 $\mu\text{g}/\text{ml}$ collagen. The mixture of cells and agarose was transferred into the μ -slide flow chamber (Ibidi) and placed in a biological safety cabinet at room temperature for 30 min to allow gelation and three-dimensional cell entrapment. The chamber was then filled with pre-warmed DMEM and incubated at 37 °C and 5 % CO_2 for 24-36 h before the experiments.

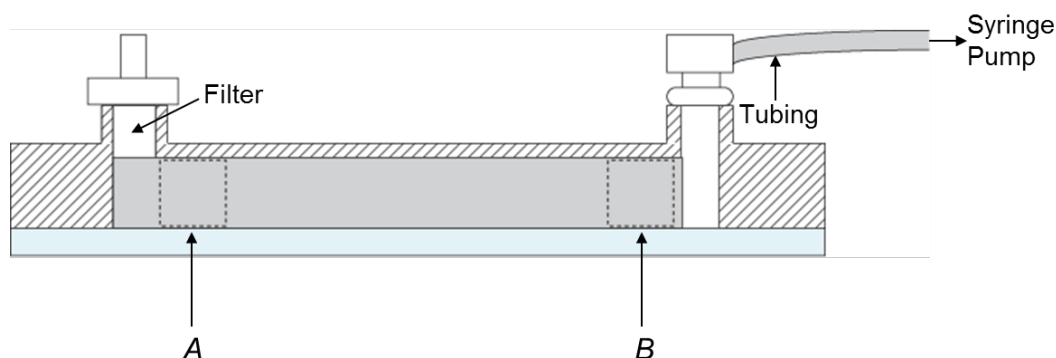


Figure 2.2 A three-dimensional (3D) cell culture chamber for imaging experiments. To examine the effect of interstitial fluid flow only on signaling activity, we observed the cells in region *A*. To examine the effect of simultaneous cell deformation/interstitial fluid flow, we observed the cells in region *B*.

2.6 Shear Flow Application and Microscopy

For imaging experiments, the inlet of the chamber containing the cell/gel construct, prepared as described above, was connected to a programmable syringe pump (Harvard Apparatus, Holliston, MA, USA), and the outlet was directly connected to a syringe filter (0.7 μm pore size; GE, Little Chalfont, Buckinghamshire, UK) to retain the scaffold under flow conditions [52] (Fig. 2.2). During experiments, the cells in the chamber were maintained in HEPES-buffered DMEM (20mM) without serum at 37 $^{\circ}\text{C}$. During imaging, dynamic, pulsed fluid flow was applied to the cells/gel construct in the chamber at 0.2 Hz (3 s on and 2 s off). Four different flow rates (2, 5, 10, or 20 $\mu\text{l}/\text{min}$) were applied to the chamber using the syringe pump (Harvard Apparatus) to explore the fluid flow-dependent mechanotransduction of FAK and Src. Images were obtained by using an automated fluorescence microscope (Nikon Instruments, Melville, NY, USA)

equipped with a charge-coupled device camera (Evolve 512; Photometrics, Tucson, AZ, USA), a filter wheel controller (Sutter Instruments, Novato, CA, USA) and a Perfect Focus System (Nikon) that maintained the focus during time-lapse imaging (Fig. 2.3). The following filter sets were used (Semrock, Rochester, NY, USA): CFP excitation: 438/24 (center wavelength/bandwidth in nm); CFP emission: 483/32; YFP (FRET) emission: 542/27. Cells were illuminated with a 100 W Hg lamp through an ND64 (~1.5% transmittance) neutral density filter to minimize photo-bleaching. Time-lapse images were acquired at an interval of 1min with a 60X (0.75 numerical aperture; Nikon) objective lens. FRET images for FAK and Src activities were generated with NIS-Elements software (Nikon) by computing emission ratio of CFP/YFP for the individual cells.

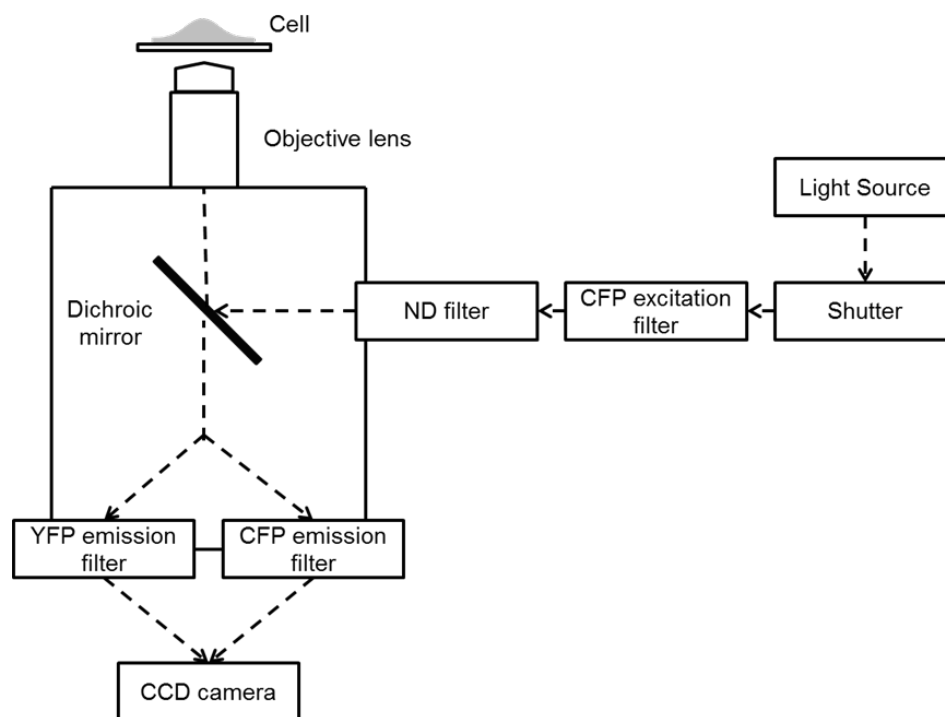


Figure 2.3 The outline of optical setup of the FRET microscope system [53]

2.7 Data Analysis and Image Processing

To see the effect of interstitial fluid flow only, FRET activity of cells at region *A* (see Fig. 2.2) was monitored. To see the effect of simultaneous cell deformation/interstitial fluid flow, the activity at region *B* (see Fig. 2.2) was monitored. Time-course activities of FAK and Src were quantified with the emission ratio of CFP/YFP. The emission ratios were normalized by the value at 0 min. The FRET images of Src and FAK activities were generated by the ImageJ software (NIH) as described previously [52]. Briefly, CFP and YFP images were background-subtracted, aligned pixel-by-pixel using a ‘MultiStackReg’ plugin, and smoothed using a median filter. The CFP images were then thresholded to convert the background pixels to ‘not a number’ (NaN), which allows elimination of artifacts in FRET ratio images resulting from the background noise. The pixel-by-pixel ratio images of CFP/YFP were generated using the ‘Ratio Plus’ plugin and ‘Blue_Green_Red’ lookup table in the ImageJ software. Finally, CFP/YFP emission ratios were normalized to the emission ratio corresponding to the basal activity of Src or FAK before flow application.

2.8 Measurement of Cell Deformation under Flow

To measure the magnitude of cell compression in two different regions (see “*A*” and “*B*” in Fig. 2.2) under flow, we obtained DIC images of the same cell before and during flow application. The cell diameter parallel to the axis of fluid flow was measured using NIS-Elements software (Nikon). The ratio of the percentage changes in cell

diameter to the original cell diameter in the direction of fluid flow was used as a measure of cell deformation.

2.9 Statistical Analysis

Data were presented as the as the mean \pm standard error of the mean (SEM). Statistical analysis was performed using Prism 5 software (GraphPad Software, La Jolla, CA, USA). Student's *t*-test was used to compare differences between two experimental groups. One-way ANOVA analysis of variance followed by Dunnett's test and Tukey's test were used to determine the statistical differences for time course experiments and multiple comparisons, respectively. The *P* value less than 0.05 was considered significant.

3. RESULTS

3.1 β 1 Integrin Activation is Significantly Enhanced in Chondrocytes in AG-Col Gel

Beta 1 integrin is known to play a critical role in cell mechanotransduction [34] and cartilage development [54]. To examine the effect of collagen crosslinking on integrin activation in C28/I2 cells seeded in AG, AG+Col, or AG-Col gels, the levels of activated and total integrin were determined by immunostaining with an activated β 1 integrin antibody, whose expression parallels the activity of β 1 integrin, and a total β 1 integrin antibody, respectively. The activated β 1 integrin level in AG-Col gel was substantially higher than that in AG and AG+Col gels (Fig. 3.1A-C). Quantification of the area of activated and total integrins in these cells was conducted. Immunofluorescence staining showed that the ratio of activated integrin normalized to that in AG gel was 280.3 % (mean) in AG-Col gels and 82.8 % in AG+Col gels, which revealed that the activated β 1 integrin level in AG-Col gels was higher than that in AG and AG+Col gels. However, the total (including both active and inactive) β 1 integrin levels were not significantly different in the three constructs. These results indicate that conjugation of type II collagen and agarose in constructs increases the activation of integrin.

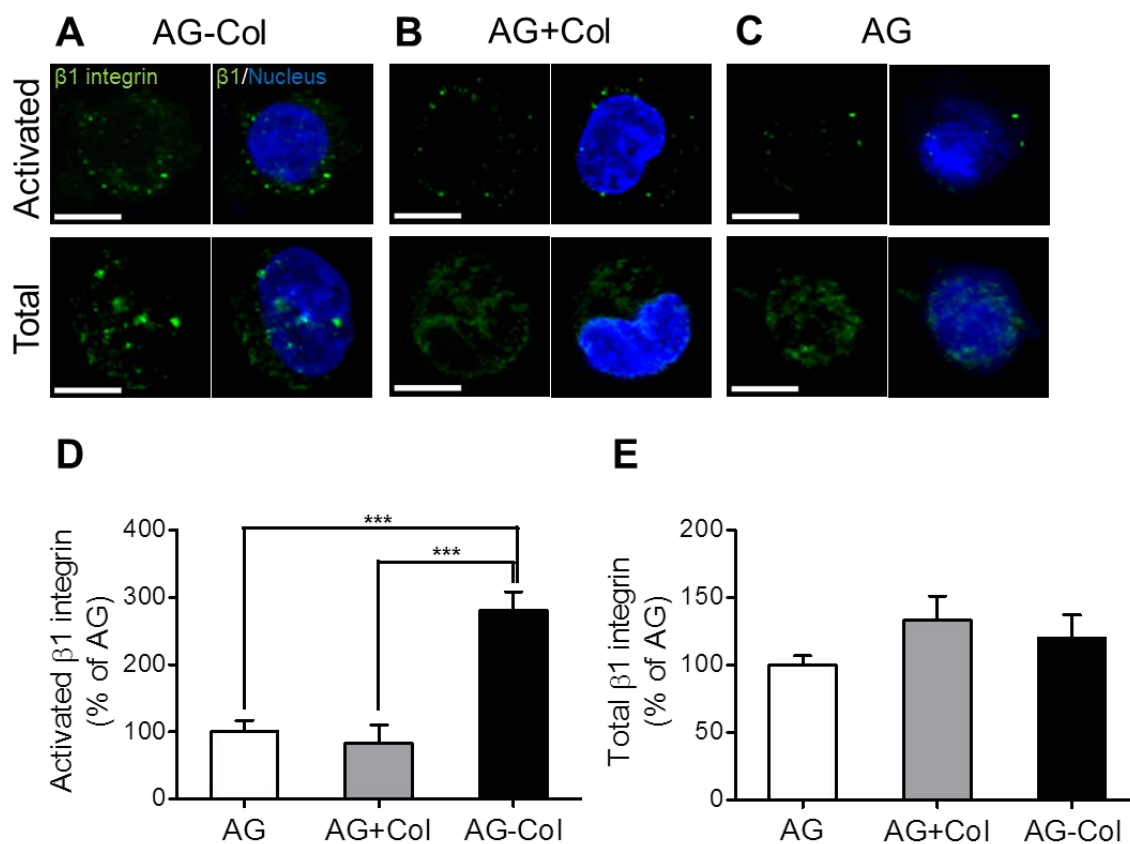


Figure 3.1 $\beta 1$ Integrin activation in C28/I2 significantly increases in AG-Col gel (A-C). Immunostaining of activated and total $\beta 1$ integrin levels in C28/I2 after seeding in AG-Col, AG+Col, and AG gels, respectively. Microphotographs are representative of 5 experiments. Scale bars: 10 μ m. (D and E) Statistical analysis of results in A, B, and C. Mean value of GFP intensity level was quantified and normalized to the averaged value in AG gel. *** $P < 0.001$. $n > 6$ cells.

3.2 Cell Deforms Substantially in Simultaneous Cell Deformation/Interstitial Fluid Flow Region

To examine the extent of cell deformation in interstitial fluid flow only region (see “A” in Fig. 2.2) and simultaneous cell deformation/interstitial fluid flow region (see “B” in Fig. 2.2), the ratio of the changes in cell diameter to the original cell diameter in the direction of fluid flow was calculated. In region A (see Fig. 2.2), the mean value of the change in cell deformation was below 1%, showing cell deformation of 0.002%, -0.008%, -0.441%, and -0.806% under 2, 5, 10, and 20 $\mu\text{l}/\text{min}$ flow rate, respectively (Fig. 3.2A). The deformation in region A in response to varying magnitudes of fluid flow was not significantly different, suggesting that cell deformation in interstitial fluid flow only region is negligible. In region B (see Fig. 2.2), substantial changes ($> 3\%$) in cell deformation were observed. The mean values of the change in cell deformation were -3.2%, -3.9%, -4.4%, and -6.1% under 2, 5, 10, and 20 $\mu\text{l}/\text{min}$ fluid flow, respectively (Fig. 3.2B). The cell deformation in response to 20 $\mu\text{l}/\text{min}$ fluid flow was significantly different from those in response to 2, 5, and 10 $\mu\text{l}/\text{min}$ fluid flow. These results implicate that the cells in region B are subjected to simultaneous cell deformation and interstitial fluid flow.

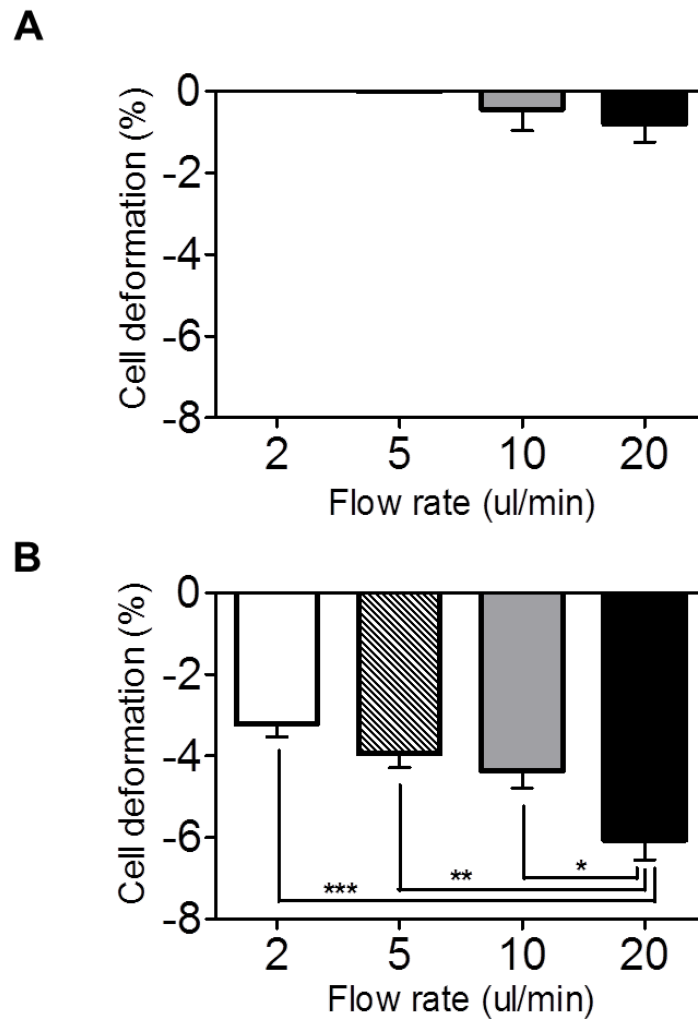


Figure 3.2 (A) The application of fluid flow at 2, 5, 10 and 20 $\mu\text{l}/\text{min}$ induced cell deformation below 1% at region “A” (see Fig. 2.2) in the 3D cell culture chamber. (B) The application of fluid flow at 2, 5, 10 and 20 $\mu\text{l}/\text{min}$ induced cell deformation above 3% at region “B” (see Fig.2). * $P < 0.05$, ** $P < 0.01$, and *** $P < 0.001$. $n > 13$ cells.

3.3 FAK Activity in Response to Interstitial Fluid Flow

To determine whether the magnitude of the interstitial fluid flow can regulate FAK activity, we transfected a FRET-based, CFP-YFP FAK biosensor into C28/I2 cells and seeded them in the AG-Col gel. Spatiotemporal changes of FAK activity were assessed by monitoring changes in the emission ratio of CFP/YFP of the FAK biosensor in the cells in the interstitial fluid flow only region. During imaging, the cells were subjected to fluid flow at 2, 5, 10 or 20 $\mu\text{l}/\text{min}$ for 1 h. For each time-lapse imaging experiment the images from the same cell were taken. FAK activity was not altered when fluid flow of 2 $\mu\text{l}/\text{min}$ was applied (Fig. 3.3A). However, in response to fluid flow at 5 $\mu\text{l}/\text{min}$, FAK inhibition ($\sim 20\%$ FRET decrease) was observed within 10 min and maintained the sustained level (Fig. 3.3B). Interstitial fluid flow at 10 $\mu\text{l}/\text{min}$ induced a transient increase of FAK activity within 2 min ($\sim 20\%$ FRET increase) and a decrease ($\sim 17\%$ FRET decrease) (Fig. 3.3C). In response to fluid flow at 20 $\mu\text{l}/\text{min}$, we observed a strong FAK activation ($\sim 17\%$ FRET increase; Fig. 3.3D) after 20 min. These substantially different activities for FAK by different magnitudes of interstitial fluid flow suggest that mechanotransduction mechanism for FAK activity might depend on the different magnitude of the applied fluid flow.

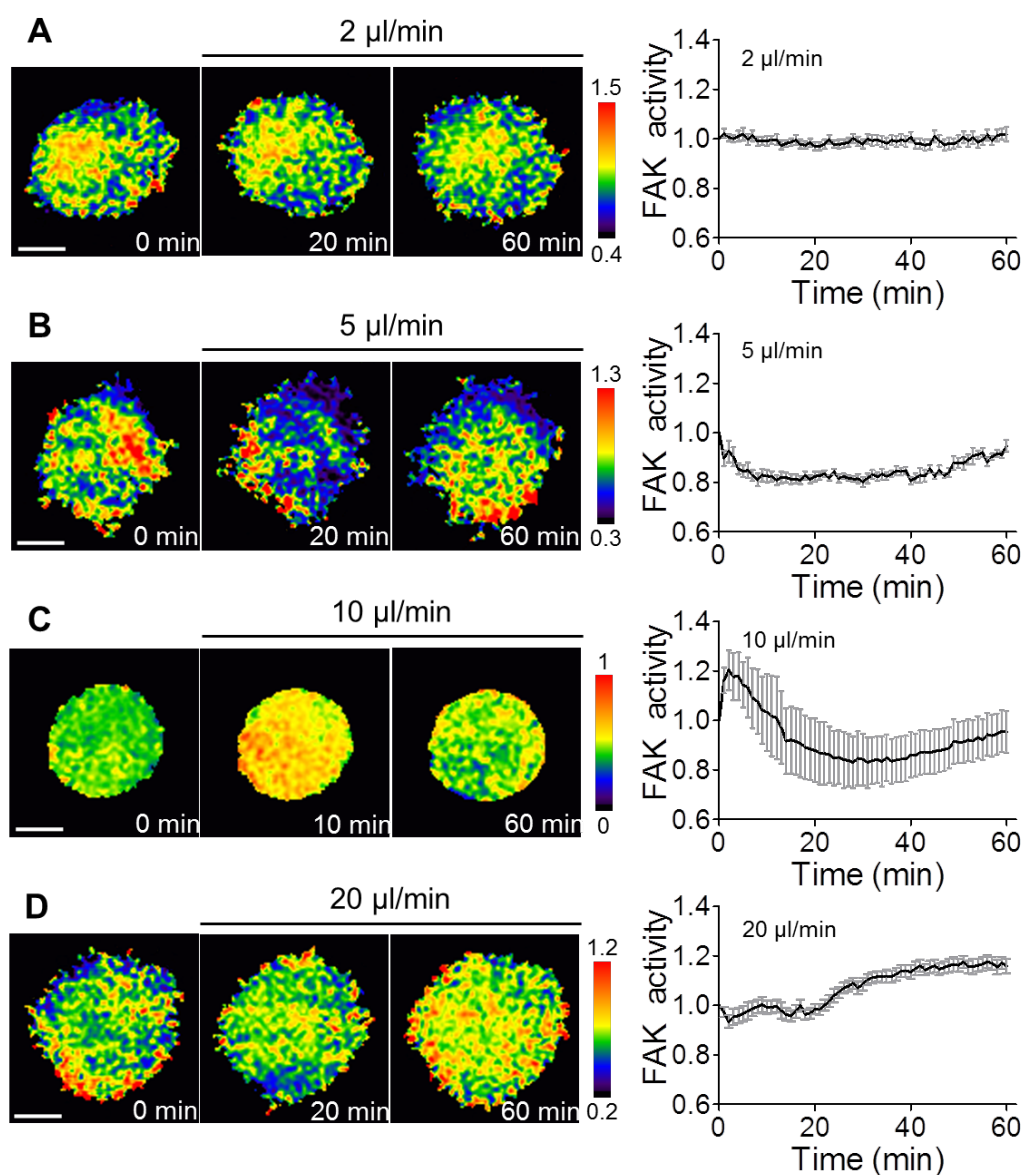


Figure 3.3 FAK activity is mechanical loading-magnitude dependent under interstitial fluid flow only. Color bar represents emission ratio of CFP/YFP of the biosensor, an index of FAK activation. Ratio images were scaled according to the corresponding color bar. CFP/YFP emission ratios were averaged over the whole cell and were normalized to time 0. (A) 2 $\mu\text{l}/\text{min}$ ($n = 12$ cells), (B) 5 $\mu\text{l}/\text{min}$ ($n = 7$ cells), (C) 10 $\mu\text{l}/\text{min}$ ($n = 6$ cells), (D) 20 $\mu\text{l}/\text{min}$ ($n = 10$ cells). Scale bars: 10 μm .

3.4 FAK Activity in Response to Simultaneous Cell Deformation/Interstitial Fluid Flow

To examine the effect of simultaneous cell deformation and interstitial fluid flow in FAK activity, C28/I2 cells were transfected with a FAK biosensor. During imaging, the cells were subjected to fluid flow at 2, 5, 10 or 20 $\mu\text{l}/\text{min}$ for 1 h and the FRET activity of a FAK biosensor was monitored at region “B” (see Fig. 2.2). In response to fluid flow at 2 $\mu\text{l}/\text{min}$ that simultaneously compressed the cell (3.2 % strain), FAK activity was maintained at the basal level (Fig. 3.4A). In response to fluid flow at 5 $\mu\text{l}/\text{min}$ with simultaneous 3.9 % compression, FAK activity decreased (~ 20 % FRET decrease) within 10 min and returned to the basal level at 60 min (Fig. 3.4B). Simultaneous application of fluid flow at 10 $\mu\text{l}/\text{min}$ and 4.4% compression resulted in a decrease in FAK activity (~ 25 % FRET decrease) within 20 min and returned to the basal level at ~ 50 min (Fig. 3.4C). Simultaneous application of fluid flow at 20 $\mu\text{l}/\text{min}$ and 6.1 % compression led to a transient decrease in FAK activity (~ 18 % FRET decrease) at 10 min followed by a rapid FAK increase (~ 22 % FRET increase) (Fig. 3.4D). These results suggest that FAK activity in response to simultaneous application of cell deformation and interstitial fluid flow is differentially regulated depending on the magnitude of loading.

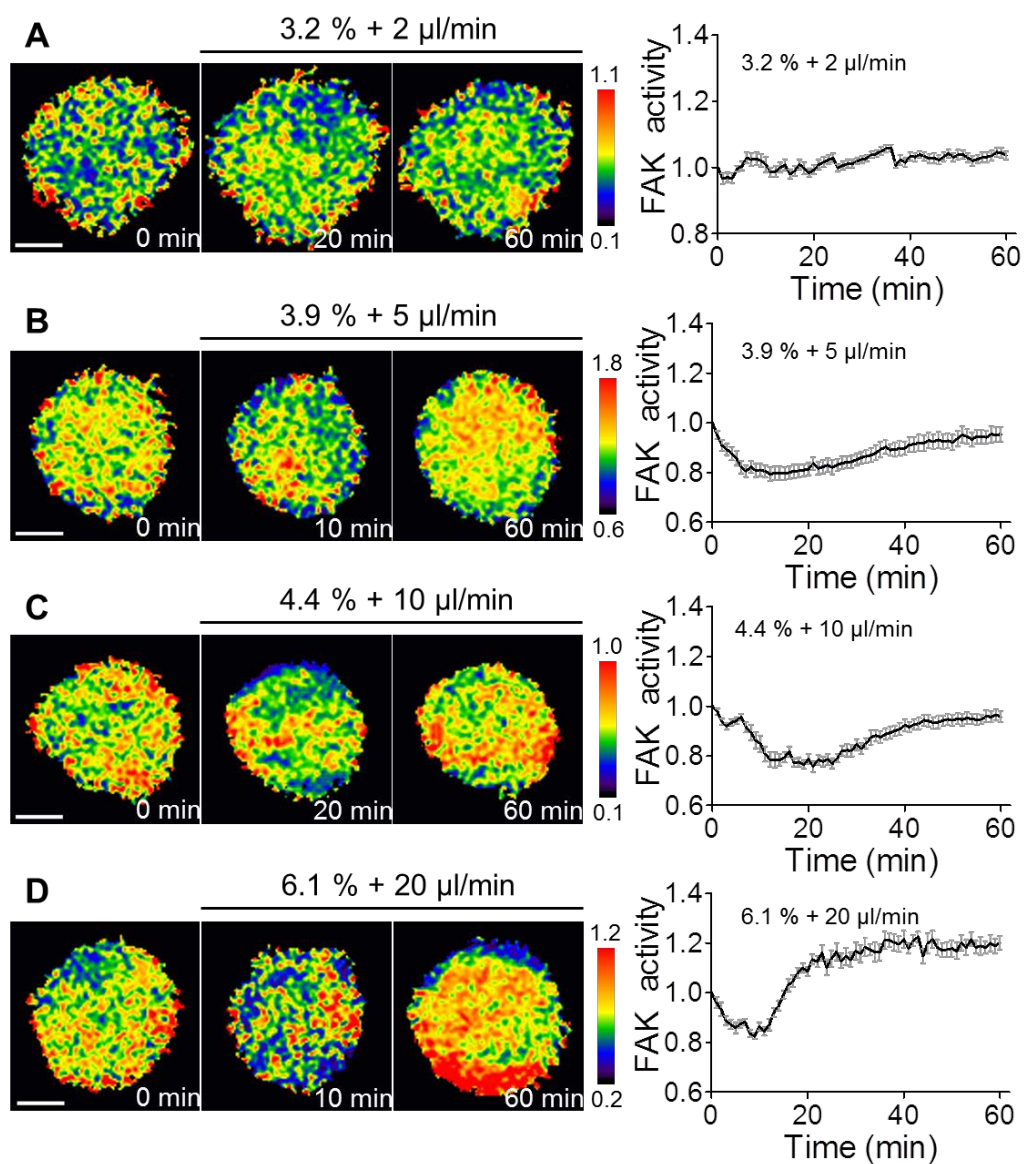


Figure 3.4 FAK activity is mechanical loading-magnitude dependent under simultaneous cell deformation and interstitial fluid flow. (A) 2 $\mu\text{l}/\text{min}$ ($n = 10$ cells), (B) 5 $\mu\text{l}/\text{min}$ ($n = 9$ cells), (C) 10 $\mu\text{l}/\text{min}$ ($n = 10$ cells), (D) 20 $\mu\text{l}/\text{min}$ ($n = 10$ cells). Scale bars: 10 μm .

3.5 Src Activity in Response to Interstitial Fluid Flow

To determine whether the magnitude of the interstitial fluid flow can regulate Src activity, we transfected C28/I2 cells with a FRET-based, CFP-YFP Src biosensor [46] and seeded them in the AG-Col gel. Spatiotemporal changes of Src activity were assessed by monitoring changes in the emission ratio of CFP/YFP of the Src biosensor in the cells in the interstitial fluid flow only region. During imaging, the cells were subjected to interstitial fluid flow at 2, 5, 10 or 20 $\mu\text{l}/\text{min}$ for 1 h. In response to 2 $\mu\text{l}/\text{min}$, Src was slightly activated, but the activation level was not significant ($\sim 3\%$ FRET increase; Fig. 3.6A). Fluid flow at 5 $\mu\text{l}/\text{min}$ inhibited Src activity ($\sim 10\%$ FRET decrease; Fig. 3.6B). In response to fluid flow at 10 $\mu\text{l}/\text{min}$, we observed a transient increase (< 3 min) in Src activity ($\sim 12\%$ FRET increase), followed by a decrease in Src activity ($\sim 15\%$ FRET decrease) at 20 min. The decreased level was maintained during flow experiments (Fig. 3.6C). Fluid flow at 20 $\mu\text{l}/\text{min}$ gradually increased Src activity and reached a maximum activation ($\sim 17\%$ FRET increase) at 30 min without the transient increase observed in 10 $\mu\text{l}/\text{min}$ flow application (Fig. 3.6D). These data indicate the dependence of Src activity on the magnitude of interstitial fluid flow.

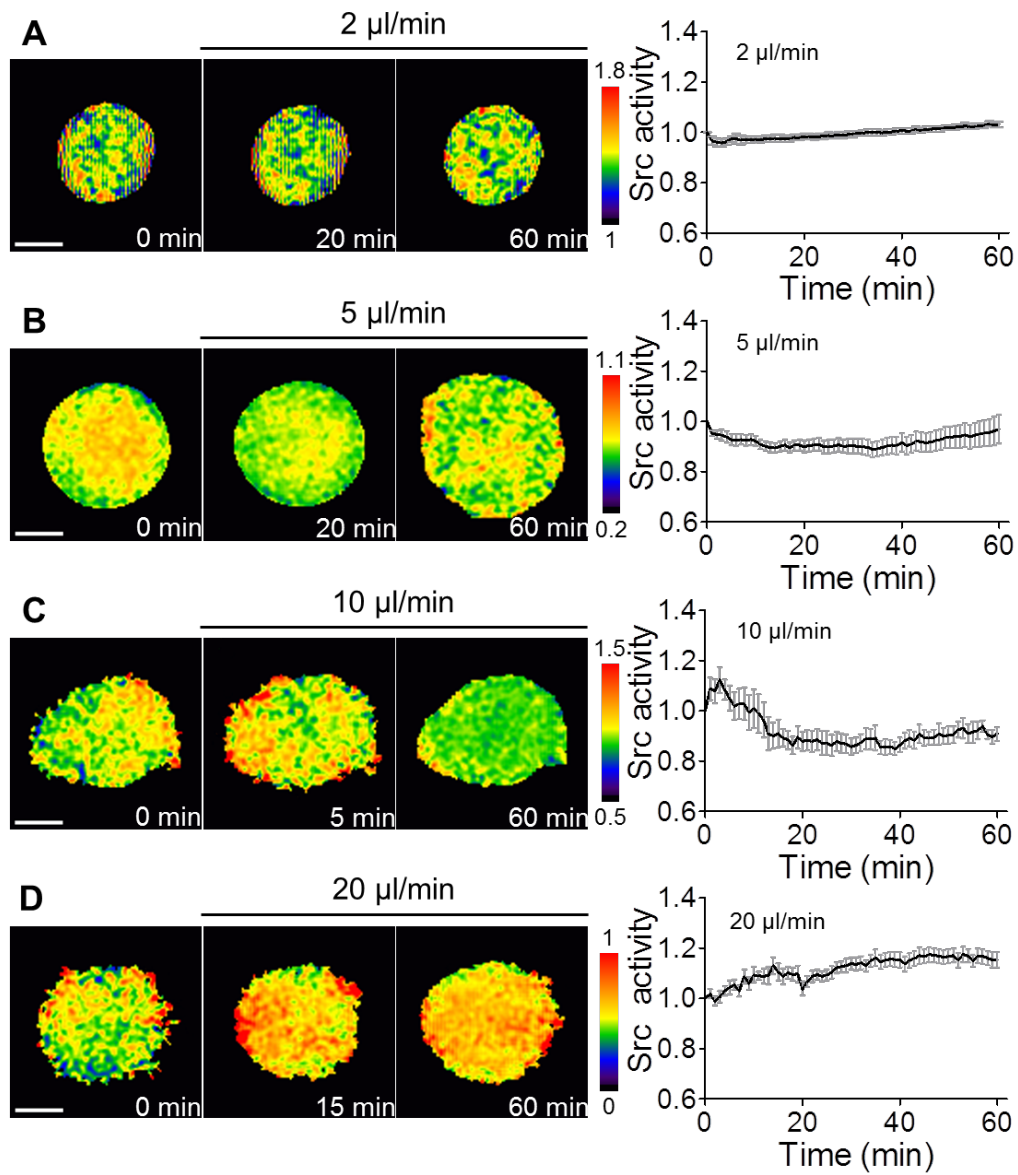


Figure 3.5 Src activity is mechanical loading-magnitude dependent under interstitial fluid flow only. (A) 2 $\mu\text{l}/\text{min}$ ($n = 4$ cells), (B) 5 $\mu\text{l}/\text{min}$ ($n = 10$ cells), (C) 10 $\mu\text{l}/\text{min}$ ($n = 7$ cells), (D) 20 $\mu\text{l}/\text{min}$ ($n = 10$ cells). Scale bars: 10 μm .

3.6 Src Activity in Response to Simultaneous Cell Deformation/Interstitial Fluid Flow

C28/I2 cells were transfected with a Src biosensor and subjected to fluid flow at 2, 5, 10 or 20 $\mu\text{l}/\text{min}$ for 1 h. During flow application, FRET imaging experiments were conducted at region “B” in the 3D culture chamber (see Fig. 2.2) to examine the effect of simultaneous application of cell deformation and interstitial fluid flow on Src activity. A significant Src activation ($\sim 14\%$ FRET increase) was observed under simultaneous application of cell compression (3.2 %) and fluid flow at 2 $\mu\text{l}/\text{min}$ (Fig. 3.6A). In response to simultaneous cell compression of 3.9 % and fluid flow at 5 $\mu\text{l}/\text{min}$, Src activity was decreased ($\sim 15\%$ FRET decrease) at 30 min and returned to the basal level at 60 min (Fig. 3.6B). In response to simultaneous cell compression of 4.4 % and interstitial fluid flow at 10 $\mu\text{l}/\text{min}$, Src activity decreased rapidly within 2 min, followed by a further decrease. At 10 min, the activity gradually increased until it reached its peak value ($\sim 19\%$ FRET increase) at 60 min (Fig. 3.6C). In response to simultaneous cell compression of 6.1 % and interstitial fluid flow at 20 $\mu\text{l}/\text{min}$, a transient Src decrease ($\sim 20\%$ FRET decrease) was observed within 10 min (Fig. 3.6D), followed by an increase ($\sim 20\%$ FRET increase) at 30 min. This dynamic Src activity under simultaneous cell compression and interstitial fluid flow at 20 $\mu\text{l}/\text{min}$ has a very similar trend to the FAK activity under the same loading condition (compare Fig. 3.6D and Fig. 3.4D).

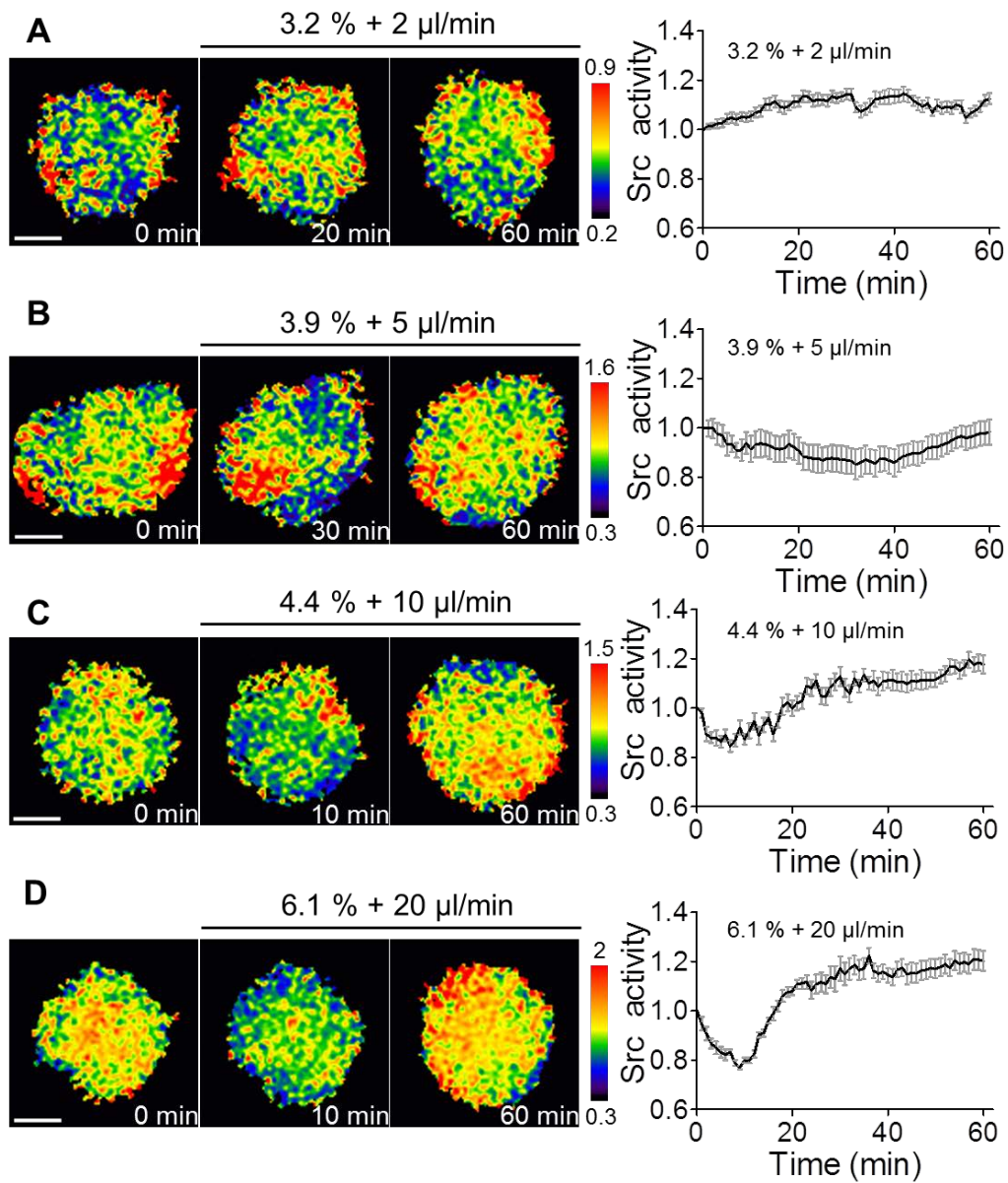


Figure 3.6 Src activity is mechanical loading-magnitude dependent under simultaneous cell deformation and interstitial fluid flow region. (A) 2 $\mu\text{l}/\text{min}$ ($n = 10$ cells), (B) 5 $\mu\text{l}/\text{min}$ ($n = 8$ cells), (C) 10 $\mu\text{l}/\text{min}$ ($n = 8$ cells), (D) 20 $\mu\text{l}/\text{min}$ ($n = 10$ cells). Scale bars: 10 μm .

3.7 Different Loading Type Does Not Affect the Loading Magnitude-Dependent FAK Activity

In this study, we hypothesized that the loading type (e.g., cell compression or interstitial fluid flow) would affect the dynamics and the level of activation of FAK and Src. To test this hypothesis, we first compared the maximal changes (e.g., maximal increase or decrease) in FAK activity under two different loading conditions: interstitial fluid flow only; and simultaneous cell compression and interstitial fluid flow (Fig, 3.7). Note that in both loading conditions interstitial fluid flow was applied. In response to fluid flow at 2 $\mu\text{l}/\text{min}$, FAK was not strongly activated (IFF: 0.2 %, Cell deformation/IFF: 2.5 %) although there was a significant difference between the two different loading conditions. Fluid flow at 5 and 10 $\mu\text{l}/\text{min}$ decreased FAK activity (IFF: -19.1 % and -16.9 %; Cell deformation/IFF: -20.5 % and -24.2 % at 5 and 10 $\mu\text{l}/\text{min}$, respectively). The activity was not significantly different between the two different loading conditions. FAK was highly activated under fluid flow at 20 $\mu\text{l}/\text{min}$ (IFF: 17.7 %; Cell deformation/IFF: 22.6 %), and the activity was not significantly different between the two loading conditions. These data demonstrate that previously observed magnitude-dependent FAK activity may not be dependent on the type of mechanical loading.

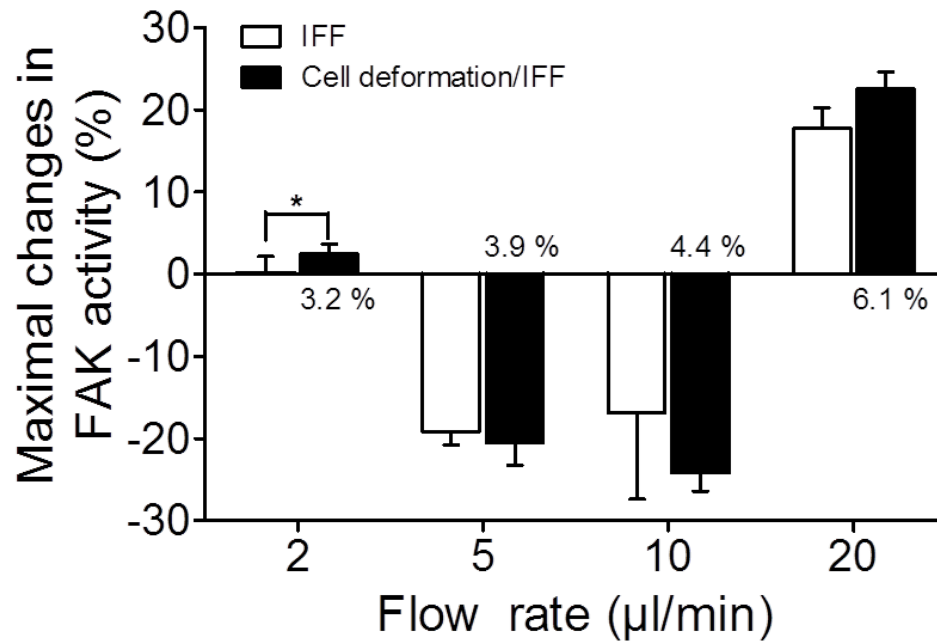


Figure 3.7 Different loading type does not affect the loading magnitude-dependent FAK activity. Bar graphs represent maximal changes in FAK activity of the cells under interstitial fluid flow only (IFF; *white*) and simultaneous cell deformation and interstitial fluid flow (Cell deformation/IFF; *black*). The numbers under black bars represent cell deformation under the given flow rate. * $P < 0.05$. $n < 6$ cells.

3.8 Different Loading Type Significantly Affects the Loading Magnitude-Dependent Src Activity

Next, we compared the maximal changes in Src activity under two different types of loading (Fig. 3.8). Simultaneous loading at 2 $\mu\text{l}/\text{min}$ significantly activated Src, but interstitial fluid flow alone did not (IFF: 3.2 %; Cell deformation/IFF: 14.5 %). Under fluid flow at 5 $\mu\text{l}/\text{min}$, both loading types significantly decreased Src activity (IFF: -10.3 %; Cell deformation/IFF: -14.8 %). Interestingly, in response to interstitial fluid flow only at 10 $\mu\text{l}/\text{min}$, Src was inhibited by -15.0 %, whereas simultaneous cell deformation (4.4 % cell compression) and interstitial fluid flow at 10 $\mu\text{l}/\text{min}$ significantly activated Src by 18.5 %. Under 20 $\mu\text{l}/\text{min}$ flow condition, both interstitial fluid flow only and simultaneous cell compression and interstitial fluid flow increased Src activity (IFF: 17.4 %; Cell deformation/IFF: 22.4 %). Together, these results suggest that Src can be differently regulated by on the type of the mechanical stimuli and cell deformation (i.e., cell compression) and interstitial fluid flow may have additive effects on Src activity.

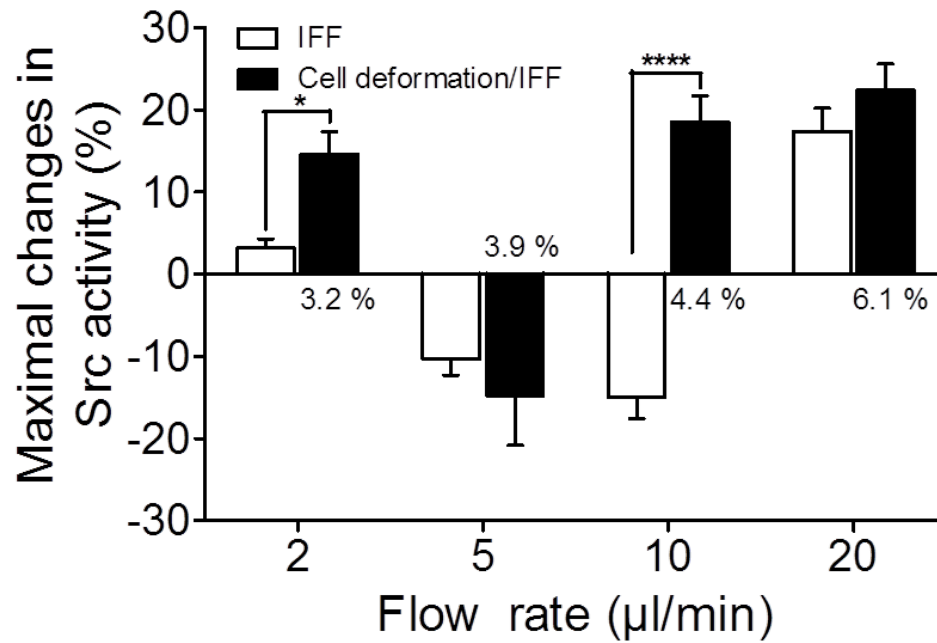


Figure 3.8 Different loading type significantly affects the loading magnitude-dependent Src activity. Bar graphs represent maximal changes in Src activity of the cells under interstitial fluid flow only (IFF; *white*) and simultaneous cell deformation and interstitial fluid flow region (Cell deformation/IFF; *black*). * $P < 0.05$, **** $P < 0.0001$. $n > 4$ cells.

3.9 FAK and Src Behave Similarly under Interstitial Fluid Flow Only

To further explore the role of interstitial fluid flow in FAK and Src activity, their activities were compared under interstitial fluid flow only at each flow rate (Fig. 3.9). Both FAK and Src were similarly increased or decreased depending on the fluid flow magnitude and the level of their activities between FAK and Src were not significantly different under the same flow conditions although their activities were significantly different in 2 $\mu\text{l}/\text{min}$ flow. These results suggest that FAK and Src respond similarly to interstitial fluid flow only and Src may be more sensitive to the low fluid flow (2 $\mu\text{l}/\text{min}$) than FAK.

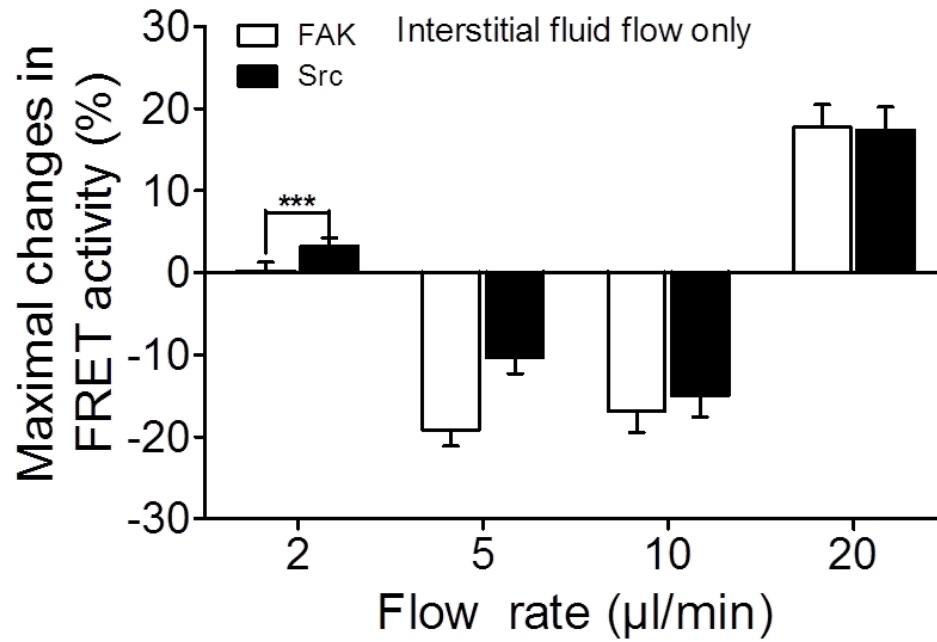


Figure 3.9 FAK and Src behave similarly under interstitial fluid flow only. Bar graphs represent maximal changes in FRET activities of FAK and Src in the cells in interstitial fluid flow only. *** $P < 0.001$. $n > 4$ cells

3.10 Simultaneous Application of Cell Deformation and Interstitial Fluid Flow Leads to Differential FAK and Src Activities

We also compared FAK and Src activities under simultaneous cell deformation and interstitial fluid flow (Fig. 3.10). In response to combined cell compression (3.2 %) and fluid flow at 2 $\mu\text{l}/\text{min}$, Src was activated more strongly than FAK was, and their difference was significant. Both FAK and Src were similarly decreased and increased under fluid flow at 5 and 20 $\mu\text{l}/\text{min}$, respectively and their maximal changes at each loading condition are not significantly different. However, simultaneous cell deformation (4.4 % cell compression) and interstitial fluid flow of 10 $\mu\text{l}/\text{min}$ contributed differently to FAK and Src activity in opposite ways. Under this loading condition, FAK was inhibited, while Src was increased. These results suggest that simultaneous cell deformation and interstitial fluid flow may lead to differential FAK and Src activities, possibly due to the additive effects of the two different types of the loading on Src activity (see Fig. 3.8).

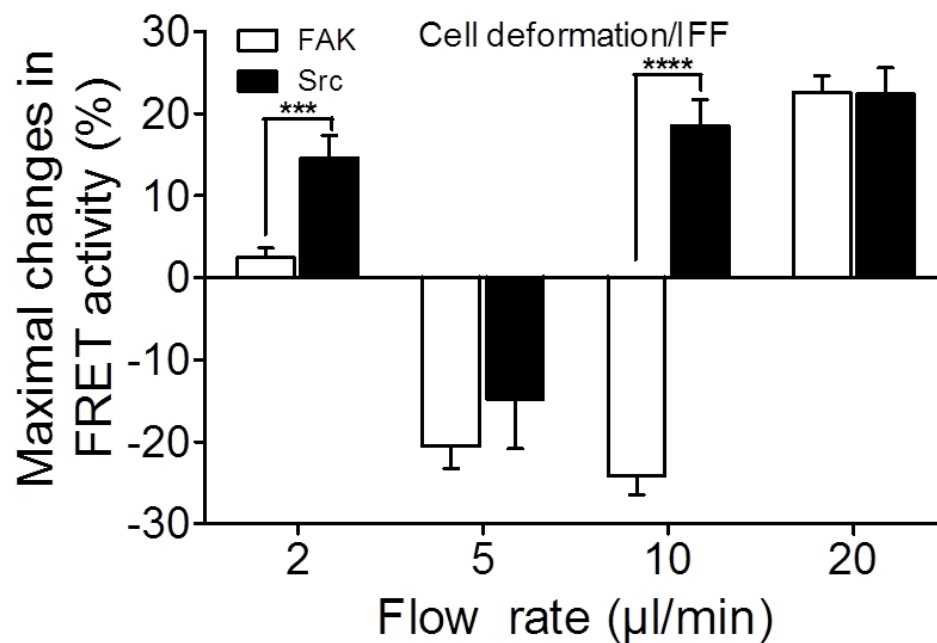


Figure 3.10 Simultaneous cell deformation and interstitial fluid flow cause differential FAK and Src activities. Bar graphs represent maximal changes in FRET activities of FAK and Src in the cells in simultaneous cell deformation/interstitial fluid flow. *** $P < 0.001$, **** $P < 0.0001$. $n > 9$ cells.

4. DISCUSSION

In this study, we used 3D gel constructs to mimic the physiologically relevant cell environment that have been shown to maintain chondrocyte phenotype and promote matrix synthesis [55, 56]. To date, many studies on the mechanotransduction of chondrocytes have been conducted in two-dimensional (2D) environment. It has been shown, for instance, that chondrocytes in 2D subjected to dynamic fluid shear stress affects cell proliferation [57]. Applying fluid shear stress in 2D has also been used to see if FAK plays an important role in mechanotransduction in osteoblasts [58]. However, chondrocytes are embedded in 3D articular cartilage *in vivo* and their response to mechanical loading in 3D has been shown to be apparently different from that in 2D [59]. Chondrocytes with a flatten morphology in monolayer culture lose their differentiated characteristics and they regain their phenotype when they are maintained in 3D environment. Internal structure of chondrocytes such as actin cytoskeleton forms differentially in 2D and 3D environment, showing a different organization or thickness of fibers [59, 60]. Expression of focal adhesion proteins such as tensin, talin, and FAK in chondrocytes is up-regulated in 3D compared to in 2D, suggesting that cell culture environment and dimensionality would distinctly affect cell signaling [60]. Moreover, 2D and 3D environments show difference in matrix production and MMP activity.

Chondrocytes promote matrix production in 3D culture by enhancing the expression of aggrecan and type II collagen [61]. Compared to 2D culture, fibroblasts grown in 3D gels produce greater expression level of MMPs, and the response of MMPs to cytokines such as TNF- α and IL-1 β is also different [62].

Using FRET-based FAK and Src biosensors, we observed that FAK and Src display distinct dynamics and activation level in C28/I2 chondrocytes depending on the magnitude of mechanical loading. Previous reports have shown that mechanical loading higher than a threshold is needed to activate the signaling proteins, while the loading lower than the threshold did not affect the proteins, suggesting the on-off switch mechanism of the cellular mechanotransduction [48, 63]. However, we showed here experimental evidence that FAK and Src activities are non-responsive, down-regulated, or up-regulated by different magnitudes of mechanical loading. This finding suggests that the signaling mechanism of FAK and Src in chondrocytes may be not be driven by a simple on-off switch, but by a loading magnitude-dependent two-level (up- or down-regulation) switch. Fluid flow of 5 and 10 $\mu\text{l}/\text{min}$ was found to down-regulate FAK activity in chondrocytes while 20 $\mu\text{l}/\text{min}$ flow up-regulated its activity. In contrast to non-responsive FAK activity under 2 $\mu\text{l}/\text{min}$ flow, Src was activated by fluid flow at 2 $\mu\text{l}/\text{min}$, suggesting that Src may be more sensitive to mechanical stimuli. Fluid flow of 5 and 20 $\mu\text{l}/\text{min}$ inhibited and enhanced Src activity in chondrocyte, respectively. This differential activity in response to varying magnitudes of mechanical loading may trigger differential MMP activity in cartilage. It was previously demonstrated that inhibited MMP activity

enhances FAK and $\beta 1$ integrin interaction in chondrogenic cell [64], but FAK promotes MMP activity in cancer cells [65, 66]. Likewise, inhibited Src activity suppresses cartilage degradation by blocking MMP activity [67]. These previous reports linking the activities of Src or FAK to MMP activity in chondrocytes support the biological significance of our data, which demonstrate the loading-magnitude dependent activities of FAK and Src.

Articular cartilage is exposed to repeated dynamic compression which simultaneously induces interstitial fluid flow, pressure gradients, and cell and matrix deformation [13]. These individual mechanical factors play important, but distinctive roles in the maintenance and remodeling of the cartilage [8, 68]. Chondrocytes in the articular cartilage, especially in the surface zone, are deformed largely by compressive loading, which simultaneously applies interstitial fluid flow to them [13, 69, 70]. This fact led us to hypothesize that, in addition to the effect of loading magnitude, chondrocytes would also be affected by the different types of mechanical loading to regulate cartilage functions. We observed herein that FAK and Src activities are differently regulated by the two types of loading – interstitial fluid flow only and simultaneous cell compression and interstitial fluid flow. Our data show that the activation level and dynamics of FAK under interstitial fluid flow only are similar to those under simultaneous cell deformation and interstitial fluid flow. In contrast, Src activity was highly dependent on the type of mechanical loading and cell compression acts as an additive effect on interstitial fluid flow-induced Src activity. Although we do

not currently know the molecular mechanism on this distinctive FAK and Src activities, our observations implicate that the different type and magnitude of mechanical loading may play distinct, but crucial roles in regulating chondrocyte mechanotransduction and MMP activities, thereby modulating cartilage homeostasis and degradation [8, 33, 51].

In summary, we have demonstrated that mechanical loading selectively activates or inhibits FAK and Src activities in loading magnitude- and type-dependent manner, and that the combined effects of interstitial fluid flow and cell deformation may selectively enhance their activities. Further studies are needed to investigate the interaction of FAK and Src under the varying magnitudes and types of mechanical loading, and how the load-induced FAK and Src activities are involved in ERK and MMP activities in chondrocytes. Our findings together with further studies on the chondrocyte mechanotransduction mechanism linking integrins-FAK/Src-ERK signaling axis and MMP activities will benefit tissue engineering as well as cartilage health.

LIST OF REFERENCES

LIST OF REFERENCES

- [1] L. C. Dijkgraaf, L. G. de Bont, G. Boering, and R. S. Liem, "The structure, biochemistry, and metabolism of osteoarthritic cartilage: a review of the literature," *J Oral Maxillofac Surg*, vol. 53, pp. 1182-92, Oct 1995.
- [2] C. J. Malemud, "Changes in proteoglycans in osteoarthritis: biochemistry, ultrastructure and biosynthetic processing," *J Rheumatol Suppl*, vol. 27, pp. 60-2, Feb 1991.
- [3] C. A. McDevitt and R. R. Miller, "Biochemistry, cell biology, and immunology of osteoarthritis," *Curr Opin Rheumatol*, vol. 1, pp. 303-14, Oct 1989.
- [4] H. B. Sun, "Mechanical loading, cartilage degradation, and arthritis," *Ann N Y Acad Sci*, vol. 1211, pp. 37-50, Nov 2010.
- [5] T. Aigner and L. McKenna, "Molecular pathology and pathobiology of osteoarthritic cartilage," *Cell Mol Life Sci*, vol. 59, pp. 5-18, Jan 2002.
- [6] T. E. Cawston and A. J. Wilson, "Understanding the role of tissue degrading enzymes and their inhibitors in development and disease," *Best Pract Res Clin Rheumatol*, vol. 20, pp. 983-1002, Oct 2006.
- [7] C. T. Hung, D. R. Henshaw, C. C. Wang, R. L. Mauck, F. Raia, G. Palmer, P. H. Chao, V. C. Mow, A. Ratcliffe, and W. B. Valhmu, "Mitogen-activated protein kinase signaling in bovine articular chondrocytes in response to fluid flow does not require calcium mobilization," *J Biomech*, vol. 33, pp. 73-80, Jan 2000.
- [8] J. B. Fitzgerald, M. Jin, D. H. Chai, P. Siparsky, P. Fanning, and A. J. Grodzinsky, "Shear- and compression-induced chondrocyte transcription requires MAPK activation in cartilage explants," *J Biol Chem*, vol. 283, pp. 6735-43, Mar 14 2008.

- [9] S. Degala, R. Williams, W. Zipfel, and L. J. Bonassar, "Calcium signaling in response to fluid flow by chondrocytes in 3D alginate culture," *J Orthop Res*, vol. 30, pp. 793-9, May 2012.
- [10] R. L. Smith, D. R. Carter, and D. J. Schurman, "Pressure and shear differentially alter human articular chondrocyte metabolism: a review," *Clin Orthop Relat Res*, pp. S89-95, Oct 2004.
- [11] R. Lane Smith, M. C. Trindade, T. Ikenoue, M. Mohtai, P. Das, D. R. Carter, S. B. Goodman, and D. J. Schurman, "Effects of shear stress on articular chondrocyte metabolism," *Biorheology*, vol. 37, pp. 95-107, 2000.
- [12] M. L. Gray, A. M. Pizzanelli, A. J. Grodzinsky, and R. C. Lee, "Mechanical and physiochemical determinants of the chondrocyte biosynthetic response," *J Orthop Res*, vol. 6, pp. 777-92, 1988.
- [13] M. Wong and D. R. Carter, "Articular cartilage functional histomorphology and mechanobiology: a research perspective," *Bone*, vol. 33, pp. 1-13, Jul 2003.
- [14] S. Degala, W. R. Zipfel, and L. J. Bonassar, "Chondrocyte calcium signaling in response to fluid flow is regulated by matrix adhesion in 3-D alginate scaffolds," *Arch Biochem Biophys*, vol. 505, pp. 112-7, Jan 1 2011.
- [15] H. Yokota, D. J. Leong, and H. B. Sun, "Mechanical loading: bone remodeling and cartilage maintenance," *Curr Osteoporos Rep*, vol. 9, pp. 237-42, Dec 2011.
- [16] T. Ikenoue, M. C. Trindade, M. S. Lee, E. Y. Lin, D. J. Schurman, S. B. Goodman, and R. L. Smith, "Mechanoregulation of human articular chondrocyte aggrecan and type II collagen expression by intermittent hydrostatic pressure in vitro," *J Orthop Res*, vol. 21, pp. 110-6, Jan 2003.
- [17] T. M. Quinn, A. J. Grodzinsky, M. D. Buschmann, Y. J. Kim, and E. B. Hunziker, "Mechanical compression alters proteoglycan deposition and matrix deformation around individual cells in cartilage explants," *J Cell Sci*, vol. 111 (Pt 5), pp. 573-83, Mar 1998.
- [18] D. A. Lee and D. L. Bader, "Compressive strains at physiological frequencies influence the metabolism of chondrocytes seeded in agarose," *J Orthop Res*, vol. 15, pp. 181-8, Mar 1997.

- [19] J. C. Shelton, D. L. Bader, and D. A. Lee, "Mechanical conditioning influences the metabolic response of cell-seeded constructs," *Cells Tissues Organs*, vol. 175, pp. 140-50, 2003.
- [20] J. J. Parkkinen, M. J. Lammi, H. J. Helminen, and M. Tammi, "Local stimulation of proteoglycan synthesis in articular cartilage explants by dynamic compression in vitro," *J Orthop Res*, vol. 10, pp. 610-20, Sep 1992.
- [21] W. B. Valhmu, E. J. Stazzone, N. M. Bachrach, F. Saed-Nejad, S. G. Fischer, V. C. Mow, and A. Ratcliffe, "Load-controlled compression of articular cartilage induces a transient stimulation of aggrecan gene expression," *Arch Biochem Biophys*, vol. 353, pp. 29-36, May 1 1998.
- [22] T. Kamiya, K. Tanimoto, Y. Tanne, Y. Y. Lin, R. Kunimatsu, M. Yoshioka, N. Tanaka, E. Tanaka, and K. Tanne, "Effects of mechanical stimuli on the synthesis of superficial zone protein in chondrocytes," *J Biomed Mater Res A*, vol. 92, pp. 801-5, Feb 2010.
- [23] S. J. Millward-Sadler, M. O. Wright, L. W. Davies, G. Nuki, and D. M. Salter, "Mechanotransduction via integrins and interleukin-4 results in altered aggrecan and matrix metalloproteinase 3 gene expression in normal, but not osteoarthritic, human articular chondrocytes," *Arthritis Rheum*, vol. 43, pp. 2091-9, Sep 2000.
- [24] J. Monfort, N. Garcia-Giralt, M. J. Lopez-Armada, J. C. Monllau, A. Bonilla, P. Benito, and F. J. Blanco, "Decreased metalloproteinase production as a response to mechanical pressure in human cartilage: a mechanism for homeostatic regulation," *Arthritis Res Ther*, vol. 8, p. R149, 2006.
- [25] H. B. Sun, R. Nalim, and H. Yokota, "Expression and activities of matrix metalloproteinases under oscillatory shear in IL-1-stimulated synovial cells," *Connect Tissue Res*, vol. 44, pp. 42-9, 2003.
- [26] H. B. Sun and H. Yokota, "Reduction of cytokine-induced expression and activity of MMP-1 and MMP-13 by mechanical strain in MH7A rheumatoid synovial cells," *Matrix Biol*, vol. 21, pp. 263-70, Apr 2002.
- [27] H. Yokota, M. B. Goldring, and H. B. Sun, "CITED2-mediated regulation of MMP-1 and MMP-13 in human chondrocytes under flow shear," *J Biol Chem*, vol. 278, pp. 47275-80, Nov 21 2003.

- [28] D. J. Leong, Y. H. Li, X. I. Gu, L. Sun, Z. Zhou, P. Nasser, D. M. Laudier, J. Iqbal, R. J. Majeska, M. B. Schaffler, M. B. Goldring, L. Cardoso, M. Zaidi, and H. B. Sun, "Physiological loading of joints prevents cartilage degradation through CITED2," *FASEB J*, vol. 25, pp. 182-91, Jan 2011.
- [29] P. A. Torzilli, M. Bhargava, S. Park, and C. T. Chen, "Mechanical load inhibits IL-1 induced matrix degradation in articular cartilage," *Osteoarthritis Cartilage*, vol. 18, pp. 97-105, Jan 2010.
- [30] J. B. Fitzgerald, M. Jin, D. Dean, D. J. Wood, M. H. Zheng, and A. J. Grodzinsky, "Mechanical compression of cartilage explants induces multiple time-dependent gene expression patterns and involves intracellular calcium and cyclic AMP," *J Biol Chem*, vol. 279, pp. 19502-11, May 7 2004.
- [31] P. M. Ragan, A. M. Badger, M. Cook, V. I. Chin, M. Gowen, A. J. Grodzinsky, and M. W. Lark, "Down-regulation of chondrocyte aggrecan and type-II collagen gene expression correlates with increases in static compression magnitude and duration," *J Orthop Res*, vol. 17, pp. 836-42, Nov 1999.
- [32] K. Honda, S. Ohno, K. Tanimoto, C. Ijuin, N. Tanaka, T. Doi, Y. Kato, and K. Tanne, "The effects of high magnitude cyclic tensile load on cartilage matrix metabolism in cultured chondrocytes," *Eur J Cell Biol*, vol. 79, pp. 601-9, Sep 2000.
- [33] R. O. Hynes, "Integrins: bidirectional, allosteric signaling machines," *Cell*, vol. 110, pp. 673-87, Sep 20 2002.
- [34] M. A. Schwartz, "Integrins and extracellular matrix in mechanotransduction," *Cold Spring Harb Perspect Biol*, vol. 2, p. a005066, Dec 2010.
- [35] J. C. Friedland, M. H. Lee, and D. Boettiger, "Mechanically activated integrin switch controls alpha5beta1 function," *Science*, vol. 323, pp. 642-4, Jan 30 2009.
- [36] E. Puklin-Faucher, M. Gao, K. Schulten, and V. Vogel, "How the headpiece hinge angle is opened: New insights into the dynamics of integrin activation," *J Cell Biol*, vol. 175, pp. 349-60, Oct 23 2006.
- [37] B. Geiger and K. M. Yamada, "Molecular architecture and function of matrix adhesions," *Cold Spring Harb Perspect Biol*, vol. 3, May 2011.

- [38] A. D. Bershadsky, N. Q. Balaban, and B. Geiger, "Adhesion-dependent cell mechanosensitivity," *Annu Rev Cell Dev Biol*, vol. 19, pp. 677-95, 2003.
- [39] K. R. Legate, S. A. Wickstrom, and R. Fassler, "Genetic and cell biological analysis of integrin outside-in signaling," *Genes Dev*, vol. 23, pp. 397-418, Feb 15 2009.
- [40] F. G. Giancotti and E. Ruoslahti, "Integrin signaling," *Science*, vol. 285, pp. 1028-32, Aug 13 1999.
- [41] C. T. Appleton, S. E. Usmani, J. S. Mort, and F. Beier, "Rho/ROCK and MEK/ERK activation by transforming growth factor-alpha induces articular cartilage degradation," *Lab Invest*, vol. 90, pp. 20-30, Jan 2010.
- [42] S. Shahrara, H. P. Castro-Rueda, G. K. Haines, and A. E. Koch, "Differential expression of the FAK family kinases in rheumatoid arthritis and osteoarthritis synovial tissues," *Arthritis Res Ther*, vol. 9, p. R112, 2007.
- [43] Y. H. Kim and J. W. Lee, "Targeting of focal adhesion kinase by small interfering RNAs reduces chondrocyte redifferentiation capacity in alginate beads culture with type II collagen," *J Cell Physiol*, vol. 218, pp. 623-30, Mar 2009.
- [44] L. Bursell, A. Woods, C. G. James, D. Pala, A. Leask, and F. Beier, "Src kinase inhibition promotes the chondrocyte phenotype," *Arthritis Res Ther*, vol. 9, p. R105, 2007.
- [45] A. Lauzier, M. Charbonneau, K. Harper, M. Jilaveanu-Pelms, and C. M. Dubois, "Formation of invadopodia-like structures by synovial cells promotes cartilage breakdown in collagen-induced arthritis: involvement of the protein tyrosine kinase Src," *Arthritis Rheum*, vol. 63, pp. 1591-602, Jun 2011.
- [46] Y. Wang, E. L. Botvinick, Y. Zhao, M. W. Berns, S. Usami, R. Y. Tsien, and S. Chien, "Visualizing the mechanical activation of Src," *Nature*, vol. 434, pp. 1040-5, Apr 21 2005.
- [47] J. Y. Seong, M. X. Ouyang, T. Kim, J. Sun, P. C. Wen, S. Y. Lu, Y. Zhuo, N. M. Llewellyn, D. D. Schlaepfer, J. L. Guan, S. Chien, and Y. X. Wang, "Detection of focal adhesion kinase activation at membrane microdomains by fluorescence resonance energy transfer," *Nature Communications*, vol. 2, Jul 2011.

- [48] S. Na, O. Collin, F. Chowdhury, B. Tay, M. Ouyang, Y. Wang, and N. Wang, "Rapid signal transduction in living cells is a unique feature of mechanotransduction," *Proc Natl Acad Sci U S A*, vol. 105, pp. 6626-31, May 6 2008.
- [49] M. C. Dodla and R. V. Bellamkonda, "Anisotropic scaffolds facilitate enhanced neurite extension in vitro," *J Biomed Mater Res A*, vol. 78, pp. 213-21, Aug 2006.
- [50] J. T. Connelly, T. A. Petrie, A. J. Garcia, and M. E. Levenston, "Fibronectin- and collagen-mimetic ligands regulate bone marrow stromal cell chondrogenesis in three-dimensional hydrogels," *Eur Cell Mater*, vol. 22, pp. 168-76; discussion 176-7, 2011.
- [51] M. B. Goldring, J. R. Birkhead, L. F. Suen, R. Yamin, S. Mizuno, J. Glowacki, J. L. Arbiser, and J. F. Apperley, "Interleukin-1 beta-modulated gene expression in immortalized human chondrocytes," *J Clin Invest*, vol. 94, pp. 2307-16, Dec 1994.
- [52] S. Wang and J. M. Tarbell, "Effect of fluid flow on smooth muscle cells in a 3-dimensional collagen gel model," *Arterioscler Thromb Vasc Biol*, vol. 20, pp. 2220-5, Oct 2000.
- [53] T. Yokono, H. Kotaniguchi, and Y. Fukui, "Clear imaging of Forster resonance energy transfer (FRET) signals of Ras activation by a time-lapse three-dimensional deconvolution system," *J Microsc*, vol. 223, pp. 9-14, Jul 2006.
- [54] A. Aszodi, E. B. Hunziker, C. Brakebusch, and R. Fassler, "Beta1 integrins regulate chondrocyte rotation, G1 progression, and cytokinesis," *Genes Dev*, vol. 17, pp. 2465-79, Oct 1 2003.
- [55] M. D. Buschmann, Y. A. Gluzband, A. J. Grodzinsky, J. H. Kimura, and E. B. Hunziker, "Chondrocytes in agarose culture synthesize a mechanically functional extracellular matrix," *J Orthop Res*, vol. 10, pp. 745-58, Nov 1992.
- [56] C. Bougault, A. Paumier, E. Aubert-Foucher, and F. Mallein-Gerin, "Molecular analysis of chondrocytes cultured in agarose in response to dynamic compression," *BMC Biotechnol*, vol. 8, p. 71, 2008.
- [57] P. Malaviya and R. M. Nerem, "Fluid-induced shear stress stimulates chondrocyte proliferation partially mediated via TGF-beta1," *Tissue Eng*, vol. 8, pp. 581-90, Aug 2002.

- [58] S. R. L. Young, R. Gerard-O'Riley, J. B. Kim, and F. M. Pavalko, "Focal Adhesion Kinase Is Important for Fluid Shear Stress-Induced Mechanotransduction in Osteoblasts," *Journal of Bone and Mineral Research*, vol. 24, pp. 411-424, Mar 2009.
- [59] P. D. Benya and J. D. Shaffer, "Dedifferentiated chondrocytes reexpress the differentiated collagen phenotype when cultured in agarose gels," *Cell*, vol. 30, pp. 215-24, Aug 1982.
- [60] R. L. Vinall, S. H. Lo, and A. H. Reddi, "Regulation of articular chondrocyte phenotype by bone morphogenetic protein 7, interleukin 1, and cellular context is dependent on the cytoskeleton," *Exp Cell Res*, vol. 272, pp. 32-44, Jan 1 2002.
- [61] S. Varghese, P. Theprungsirikul, S. Sahani, N. Hwang, K. J. Yarema, and J. H. Elisseeff, "Glucosamine modulates chondrocyte proliferation, matrix synthesis, and gene expression," *Osteoarthritis Cartilage*, vol. 15, pp. 59-68, Jan 2007.
- [62] W. R. Wong, S. Kossodo, and I. E. Kochevar, "Influence of cytokines on matrix metalloproteinases produced by fibroblasts cultured in monolayer and collagen gels," *J Formos Med Assoc*, vol. 100, pp. 377-82, Jun 2001.
- [63] Y. C. Poh, S. Na, F. Chowdhury, M. Ouyang, Y. Wang, and N. Wang, "Rapid activation of Rac GTPase in living cells by force is independent of Src," *PLoS One*, vol. 4, p. e7886, 2009.
- [64] E. J. Jin, Y. A. Choi, E. Kyun Park, O. S. Bang, and S. S. Kang, "MMP-2 functions as a negative regulator of chondrogenic cell condensation via down-regulation of the FAK-integrin beta1 interaction," *Dev Biol*, vol. 308, pp. 474-84, Aug 15 2007.
- [65] P. M. Siesser and S. K. Hanks, "The signaling and biological implications of FAK overexpression in cancer," *Clin Cancer Res*, vol. 12, pp. 3233-7, 2006.
- [66] M. H. Wu, J. F. Lo, C. H. Kuo, J. A. Lin, Y. M. Lin, L. M. Chen, F. J. Tsai, C. H. Tsai, C. Y. Huang, and C. H. Tang, "Endothelin-1 promotes MMP-13 production and migration in human chondrosarcoma cells through FAK/PI3K/Akt/mTOR pathways," *J Cell Physiol*, vol. 227, pp. 3016-26, 2012.

- [67] B. C. Sondergaard, N. Schultz, S. H. Madsen, A. C. Bay-Jensen, M. Kassem, and M. A. Karsdal, "MAPKs are essential upstream signaling pathways in proteolytic cartilage degradation--divergence in pathways leading to aggrecanase and MMP-mediated articular cartilage degradation," *Osteoarthritis Cartilage*, vol. 18, pp. 279-88, Mar 2010.
- [68] R. L. Kane, K. J. Saleh, T. J. Wilt, B. Bershadsky, W. W. Cross, 3rd, R. M. MacDonald, and I. Rutks, "Total knee replacement," *Evid Rep Technol Assess (Summ)*, pp. 1-8, Dec 2003.
- [69] A. D. Pearle, R. F. Warren, and S. A. Rodeo, "Basic science of articular cartilage and osteoarthritis," *Clin Sports Med*, vol. 24, pp. 1-12, Jan 2005.
- [70] D. R. Carter, G. S. Beaupre, M. Wong, R. L. Smith, T. P. Andriacchi, and D. J. Schurman, "The mechanobiology of articular cartilage development and degeneration," *Clin Orthop Relat Res*, pp. S69-77, Oct 2004.